

UNCLASSIFIED

DTIC FILE COPY

12

AD-A183 703

SECURITY CLASSIFICATION OF THIS PAGE (When Data Entered)

REPORT DOCUMENTATION PAGE		READ INSTRUCTIONS BEFORE COMPLETING FORM
1. REPORT NUMBER ONR NR 659-819/7/87	2. GOVT ACCESSION NO.	3. RECIPIENT'S CATALOG NUMBER
4. TITLE (and Subtitle) INFRARED MULTIPHOTON DISSOCIATION OF RDX IN A MOLECULAR BEAM		5. TYPE OF REPORT & PERIOD COVERED TECHNICAL REPORT
		6. PERFORMING ORG. REPORT NUMBER
7. AUTHOR(s) Xinsheng Zhao, Eric J. Hints, and Yuan T. Lee		8. CONTRACT OR GRANT NUMBER(s) N00014-83-K-0069 NR 659-819
9. PERFORMING ORGANIZATION NAME AND ADDRESS Professor Yuan T. Lee Dept. of Chemistry, Univ. of California Berkeley, California 94720		10. PROGRAM ELEMENT, PROJECT, TASK AREA & WORK UNIT NUMBERS
11. CONTROLLING OFFICE NAME AND ADDRESS Dr. Richard S. Miller, Office of Naval Research Dept. of the Navy, Office of Naval Research 800 N. Quincy Street, Arlington, VA 22217		12. REPORT DATE July 7, 1987
		13. NUMBER OF PAGES 40
14. MONITORING AGENCY NAME & ADDRESS (if different from Controlling Office) Office of Naval Research-Resident Representative UCB Residency, Richmond Field Station Univ. of Calif., Berkeley, Calif. 94720		15. SECURITY CLASS. (of this report) Unclassified
		15a. DECLASSIFICATION/DOWNGRADING SCHEDULE
16. DISTRIBUTION STATEMENT (of this Report) Submitted to Journal of Chemical Physics Unlimited		
<div style="border: 1px solid black; padding: 5px; display: inline-block;"> <b>DISTRIBUTION STATEMENT A</b>            Approved for public release            Distribution Unlimited         </div>		
17. DISTRIBUTION STATEMENT (of the abstract entered in block 20, if different from Report)		
18. SUPPLEMENTARY NOTES None		
19. KEY WORDS (Continue on reverse side if necessary and identify by block number) RDX, energetic materials, solid propellants, unimolecular decomposition, concerted reactions.		
20. ABSTRACT (Continue on reverse side if necessary and identify by block number) (See reverse side)		

DTIC  
ELECTE  
AUG 25 1987

S D

DD FORM 1 JAN 73 1473

EDITION OF 1 NOV 85 IS OBSOLETE  
S/N 0102-LF-014-6601

UNCLASSIFIED

SECURITY CLASSIFICATION OF THIS PAGE (When Data Entered)

## 20. ABSTRACT

Infrared multiphoton dissociation (IRMPD) of hexahydro-1,3,5-trinitro-1,3,5-triazine (RDX) in a molecular beam has been performed in order to investigate the mechanism of RDX thermal decomposition. A beam of molecules was crossed by a pulsed TEA  $\text{CO}_2$  laser and velocity distributions of the various products were measured by the time-of-flight (TOF) technique as a function of the laboratory angle using a mass spectrometric detector. The dissociation channels, their branching ratios, and the translational energy distributions of the the products were determined. In contrast to the conventional view of simple bond rupture through loss of  $\text{NO}_2$  as the dominant primary channel in RDX decomposition, it was found that the dominant primary channel is concerted symmetric triple fission to produce three  $\text{CH}_2\text{N}_2\text{O}_2$  fragments which subsequently undergo secondary concerted dissociation to produce HCN,  $\text{H}_2\text{CO}$ , HONO (or  $\text{HNO}_2$ ) and  $\text{N}_2\text{O}$ . A total of two primary and four secondary dissociation channels were observed. Concerted reactions predominate over simple bond rupture not only in the number of channels (four vs. two) but also in the amount of products. A fair amount of translational energy release through concerted reaction channels was observed, which is significant for an explanation of the energetics of RDX decomposition.



fragments which subsequently undergo secondary concerted dissociation to produce HCN, H<sub>2</sub>CO, HONO (or HNO<sub>2</sub>) and N<sub>2</sub>O. A total of two primary and four secondary dissociation channels were observed. Concerted reactions predominate over simple bond rupture not only in the number of channels (four vs. two) but also in the amount of products. A fair amount of translational energy release through concerted reaction channels was observed, which is significant for an explanation of the energetics of RDX decomposition.

## I. INTRODUCTION

Hexahydro-1,3,5-trinitro-1,3,5-triazine (RDX) is a relatively stable energetic compound which releases a large amount of energy in bulk decomposition. One of the interesting results from experimental studies of the thermal decomposition of RDX is that the observed products are almost exclusively simple molecules such as HCN, N<sub>2</sub>O, H<sub>2</sub>CO, H<sub>2</sub>O, NO<sub>2</sub>, NO, CO<sub>2</sub>, and CO. What the primary initiation and secondary decomposition processes are which lead to the formation of a variety of simple stable molecules and how the stored energy is released in decomposition have been two of the most important questions concerning the decomposition of RDX. Although RDX has been studied extensively for several decades both experimentally and theoretically,<sup>1-4</sup> the above questions are still unanswered.

It has been recognized that the decomposition of bulk RDX is a very complicated process involving both unimolecular and bimolecular reactions. It was commonly believed that the most probable initial decomposition step was simple bond rupture which eliminates NO<sub>2</sub> from RDX, since the weakest bond in RDX is the N-N bond. But this picture is far from conclusive, and other possible mechanisms including unimolecular simple bond rupture or concerted dissociation as well as several bimolecular reactions between RDX molecules have been proposed. The crucial obstacle to the understanding of RDX decomposition has been the lack of an effective experimental tool to "follow" the primary and secondary elementary reactions directly.

Infrared multiphoton dissociation (IRMPD) of molecules in a molecular beam and measuring product angular and velocity distributions has proven to be an ideal method to study unimolecular "thermal" decomposition of polyatomic molecules under isolated conditions.<sup>5-7</sup> It has been shown that for molecules which are moderate in size, the lifetime of the infrared-multiphoton-excited molecule is long enough to allow vibrational energy randomization before dissociation, and the same dissociation mechanism is observed for IRMPD as for thermal decomposition. The fact that we can "thermally heat" the isolated molecule in a molecular beam offers a greatly simplified environment for the investigation of unimolecular reactions without any complication from secondary bimolecular reactions of primary products. Measurements of angular and velocity distribution of fragments under collision-free condition are not only important for the understanding of dissociation dynamics but also essential for the unambiguous identification of the primary products. Even if the products do not yield their parent ions during the electron impact ionization, using the requirement of momentum conservation in the center of mass (C.M.) coordinate system to match the velocity distributions of various products, it is possible to determine the dissociation channels and their branching ratios as well as the translational energy distribution,  $P(E_T)$ , of the products.

In a series of studies on the decomposition of ethers<sup>6</sup> and nitroalkanes<sup>7</sup>, it has been clearly shown that because of the different dissociation dynamics, concerted dissociation and simple bond rupture can be distinguished easily from the observed translational energy

distributions. In the case of simple bond rupture there is no appreciable exit barrier along the reaction coordinate so that the final translational energy distribution of products is closely related to the energy distribution in the reaction coordinate. For molecules with many vibrational degrees of freedom which share internal energy statistically, only a small amount of translational energy is released with the peak of the  $P(E_T)$  almost at zero translational energy. In contrast, concerted dissociation has a substantial exit barrier, and upon overcoming this barrier the products have to carry away this potential energy. It is found<sup>7</sup> that the repulsion between products dominates the dissociation dynamics and about half of this exit barrier energy appears in translation. As a result, the average translational energy is usually substantially higher than that of simple bond rupture and the peak of the  $P(E_T)$  is far away from zero translational energy. Because of the complication caused by the excessive fragmentation of product molecules in the electron bombardment ionizer the unique relation between dissociation dynamics and mechanism will be shown to play an important role in the elucidation of the dissociation mechanism of RDX.

In this paper, results of experimental studies on the IRMPD of RDX in a molecular beam are presented. The reaction mechanism which best explains the experimental observations is proposed. It is found that the symmetrical fission of RDX into three  $\text{CH}_2\text{NNO}_2$  fragments is the dominant primary channel, and the subsequent concerted dissociations of  $\text{CH}_2\text{NNO}_2$  are found to be responsible for the production of such small

molecules as HCN,  $N_2O$ ,  $H_2CO$  and HONO. N-N bond rupture leading to the elimination of  $NO_2$  is also found to occur, but this is only a minor primary channel.

## II. EXPERIMENTAL ARRANGEMENT

The experimental apparatus was basically the same as that described elsewhere.<sup>8</sup> Two modifications were made for this experiment. 1) The molecular beam source in fig. 1 of ref. 8 was replaced by a new oven composed of two parts, a reservoir which held RDX and a forward nozzle chamber on which there was a 1 mm diameter nozzle. The oven was sandwiched between two metal mounting plates which were welded to the back flange of the source chamber. Six pins were used to kinematically mount the oven at the correct position, three above, spring loaded to apply pressure, and three below, engaged in T shaped V grooves on the bottom of the oven to assure the positive alignment of the nozzle when the oven was heated. 2) A single skimmer, mounted on the wall of the source chamber, was located 2.5 cm from the nozzle and was heated to about 200°C in order to prevent the condensation of RDX on the skimmer. This skimmer and the slit of the oven were used as the beam defining elements and the usual skimmer between the differential and main chambers was removed.

For producing the beam of RDX, the reservoir of the oven, in which RDX was loaded before the machine was evacuated, was heated to 130°C at

which the vapor pressure of RDX is estimated to be about 0.1 torr, and the temperature of the nozzle was kept at 154°C. He (99.995 per cent) carrier gas at 50 torr was led into the oven, then the mixture of He and RDX was expanded into the source chamber through the nozzle to produce an intense supersonic beam. The beam of RDX with a mean velocity of  $1.2 \times 10^5$  cm/sec and a 13 per cent FWHM velocity spread was then crossed with the beam of a pulsed  $\text{CO}_2$  laser in the interaction region of the main chamber. RDX molecules in the beam were excited through IR multiphoton excitation (IRMPE) processes above the dissociation energy causing decomposition of the excited molecules. The dissociation fragments were detected by a mass spectrometer at specified laboratory angles with respect to the direction of the molecular beam which is variable by rotating the entire molecular beam source chamber about the laser propagation axis. The time-resolved mass spectrometric signals, time-of-flight (TOF) spectra, triggered by laser pulse were recorded at all mass to charge ratios (m/e) in which dissociation products were detectable for the analysis of product velocity distributions.

A GENTEC DD-250 TEA  $\text{CO}_2$  laser was used as the MPD laser, and the P22 line of  $10^00-00^01$  transition (at 10.6 $\mu\text{m}$ ) was chosen for excitation. The laser beam was focused to 1 mm diameter at the crossing point of the two beams. The temporal length of the laser pulse was around 600 ns, and two repetition rates of 30 Hz and 100 Hz were used at various times. Laser fluences of 6 J/cm<sup>2</sup> to 20 J/cm<sup>2</sup> per pulse were used.

For a more detailed description of the machine and operating conditions as well as the technique of recording the TOF spectra refs. 7 and 8 are recommended. The RDX obtained from the Lawrence Livermore National Laboratory was used in this experiment without purification.

### III. RESULTS

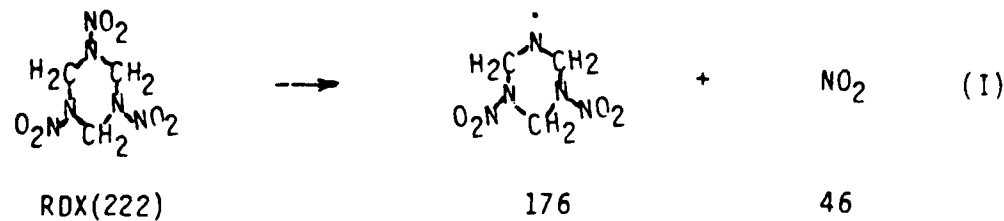
Prior to the photolysis experiment, the mass spectrum of RDX in the molecular beam was taken at various temperatures. Using a small (0.1 mm diameter) entrance slit on the detector, the laboratory angle of the molecular beam was set to zero, the direction of the detector, and the molecular beam was pointed straight into the detector allowing the beam of RDX molecules to be detected directly using electron bombardment ionization followed by a quadrupole mass spectrometer. The temperature of the reservoir was maintained at 170°C, and the temperature of the nozzle was varied from 170°C upwards. Without the carrier gas, by using a spinning slotted disk to measure the TOF spectrum of the effusive beam at  $m/e = 30$  ( $\text{NO}^+$ ) it was found that the TOF distribution was exactly that expected from stable RDX at the nozzle temperature when the temperature was below 200°C. When the temperature of the nozzle was raised above 200°C a fast component from dissociation products appeared. The fast peak due to dissociation became substantial when the nozzle was heated to 220°C. These observations imply that the rate of thermal decomposition of RDX is slow at temperatures below 200°C. The mass spectrum of RDX above  $m/e = 28$  contains all the masses reported by Farber and Srivastava,<sup>9</sup> with one significant difference. While Farber

and Srivastava claimed that the RDX molecule does not appear in the gas phase, in this experiment not only parent ion with  $m/e = 222$  was detected but also, as mentioned above, below  $200^{\circ}\text{C}$  the effusive beam from the oven consisted almost entirely of stable RDX molecules. The observed mass spectrum of RDX contains peaks of  $m/e = 222, 148, 132, 120, 102, 81-83, 74, 56, 46, 44, 42, 30, 26-28,$  and  $12-16$ , but not  $175$  nor  $176$ .

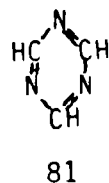
Products from laser photolysis were detected and TOF spectra were obtained at  $m/e = 120, 119, 102, 80-82, 74, 56, 46, 44, 42, 26-30,$  and  $12-17$ . Signals at  $m/e$  of  $119$ , and both  $82$  and  $80$  were found to be the same as those at  $120$  and  $81$  respectively. Very weak signal at  $m/e = 83$  was observed, but it was too weak to be used for data analysis. A very careful scan between  $m/e = 120$  and  $222$  was performed, but no signal was detected within this range. For  $m/e = 120, 102, 81, 74$  and  $30$ , TOF spectra at different laboratory angles were collected, while for other  $m/e$ 's only one laboratory angle was chosen. Figures 1 and 2 show these TOF spectra with the fit using the mechanism presented in the next section. Most of these spectra were taken at a laser power of  $20 \text{ J/cm}^2$  and it was found that within the range of laser powers of this experiment ( $6 - 20 \text{ J/cm}^2$ ) the shapes of the TOF spectra showed no significant differences.

#### IV. ANALYSIS

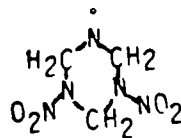
Although  $m/e = 176$  was not detected (notice that even RDX itself gives no  $m/e = 176$  fragment in the mass spectrum) the existence of reaction (I)



is evident. TOF spectra at  $m/e = 120$  and  $102$  have the same velocity distribution whose most probable velocity is almost the same as that of the molecular beam, showing that these fragments which have very small average recoil energies are produced from a simple bond rupture channel. The TOF spectra at  $m/e = 80 - 82$  also contain this component, implying that these ions are daughter ions of one primary product. A possible formula of  $120$  (hereafter the molecular weight in amu is used to represent the related species) is  $\text{CH}_2\text{N}_3\text{O}_4^+$ , and those of  $102$  are  $\text{C}_2\text{H}_4\text{N}_3\text{O}_2^+$  or  $\text{CH}_2\text{N}_4\text{O}_2^+$ , while the fragments around  $81$  must consist of the ring frame of RDX:

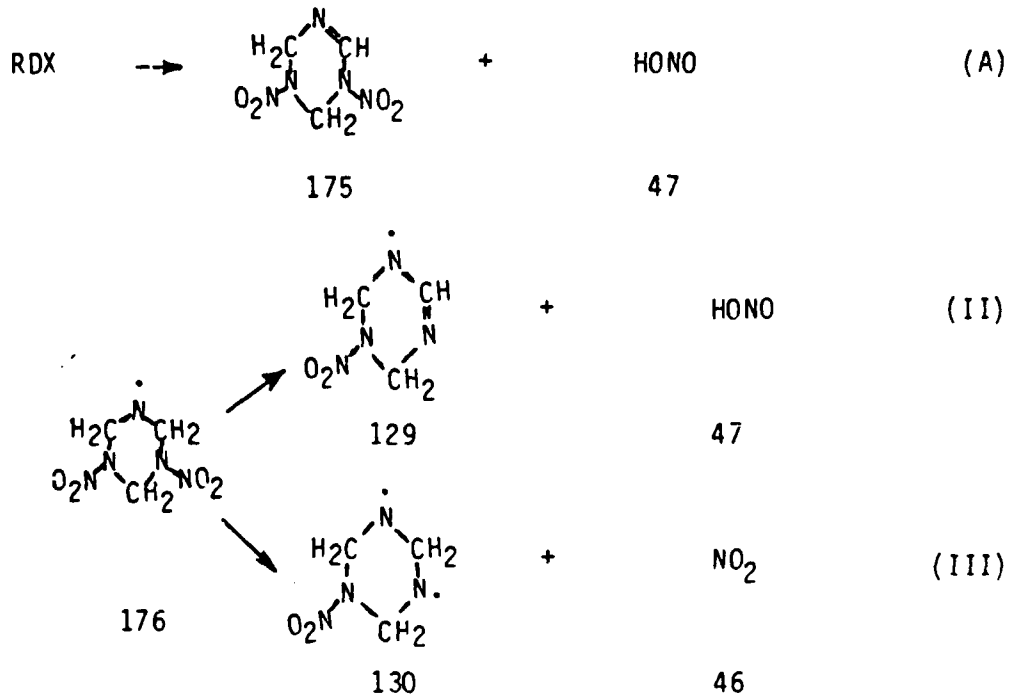


Therefore the common parent product must be



By fitting the TOF spectrum of  $m/e = 120$  using reaction (I), a product translational energy distribution was obtained which is typical for simple bond rupture and is presented in figure 3.

The TOF spectrum of  $m/e = 81$  contains at least one more faster component. Possible products which give faster  $m/e=81$  component could come from the following reactions



It is also possible that 129, 130 and 175 undergo further dissociation by eliminating one or two NO<sub>2</sub> or HONO molecules and contribute to the  $m/e = 81$  signal.

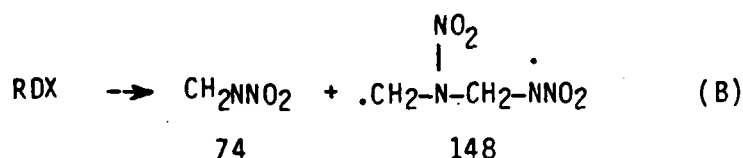
Because 175 has a similar ring structure to that of 176, we expect that if reaction (A) took place, the faster  $m/e = 81$  component would have also appeared in the TOF spectrum of  $m/e = 120$  and 102, but it did not. The second product of reaction (A), HONO, does not yield parent ion ( $m/e=47$ ) but it is the only fragment which produces OH<sup>+</sup> ( $m/e = 17$ ). We have tried to match both the faster component of  $m/e = 81$  and 17 assuming

they were from reaction (A), but the  $m/e = 17$  signal is too slow to match the fast component in the  $m/e = 81$  TOF spectrum by momentum conservation, showing that reaction (A) is not a major channel.

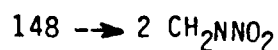
Since reaction (A) cannot be compatible with our experimental results, reaction (II) becomes the next likely candidate to explain the TOF spectra of both  $m/e = 81$  and 17. If the fast component in the  $m/e = 81$  TOF spectrum is from 129 produced from 176 product through reaction (II), by conservation of linear momentum in the dissociation of 176 we should be able to fit both the fast components in the TOF spectra of  $m/e = 81$  and 17 as a pair of products with mass numbers 129 and 47. In figures 1 and 2 both fast parts of the TOF spectra of  $m/e=81$  and 17 shown as dash-dot curves are matched very well with each other assuming they are produced from the secondary dissociation of primary product 176 through reaction (II) using the  $P(E_T)$  presented in figure 4. The fact that the  $P(E_T)$  shown in figure 4 has a substantially higher average energy than that of reaction (I) and peaks away from zero implies that the products are from a concerted reaction, which is consistent with reaction (II). In order to perfectly fit the TOF spectrum of  $m/e = 81$  another component with a velocity distribution between those of 176 and 129 is needed. The same problem occurs for fitting  $m/e = 56$  (with the possible formula  $C_2H_4N_2^+$ ) and especially 42 (with the possible formulas  $C_2H_4N^+$  or  $CH_2NN^+$ ). After reaction (III) is considered, all these problems disappear immediately. Figure 5 shows the  $P(E_T)$  for reaction (III) which is again consistent with simple bond rupture.

We can not absolutely rule out the possibility that the TOF spectrum of  $m/e = 81$  could contain other products besides those from reactions (I), (II) and (III), but since the data analysis assuming only reactions (I)-(III) gives satisfactory results we believe that other reaction channels whose products would appear at  $m/e = 81$  are not significant.

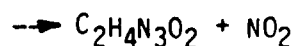
The TOF of  $m/e = 74$  definitely differs from those with higher mass numbers. Farber and Srivastava suggested the following reaction channel<sup>9</sup>



to explain the  $m/e = 74$  peak they observed in the mass spectrometer, but in our experiment no trace of  $m/e = 148$  was detected although the  $m/e = 148$  peak is quite strong in the mass spectrum of RDX. Even if 148 was produced but was internally hot so that it would not survive in the ionizer, we should still be able to see the contribution of 148 at its fragment masses, especially at  $m/e = 74$  which would show slow peak obviously different from 74 itself in the TOF. If 148 from (B) underwent secondary dissociation as



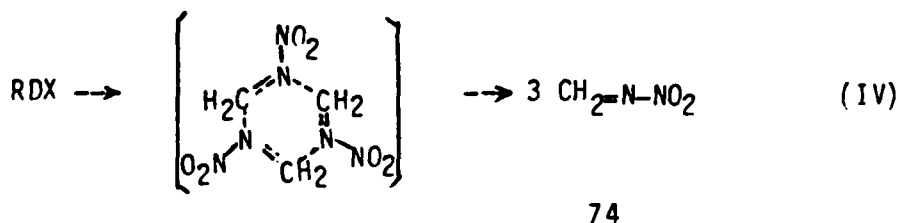
or



(C)

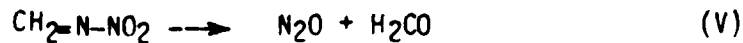
we should be able to detect these products at their characteristic fragmentation pattern and velocity distributions, but no evidence was

found. Because there is no trace of 148 or its fragments and the fact that the  $m/e = 74$  TOF spectrum is quite fast, which is inconsistent with a simple bond rupture reaction, the  $m/e = 74$  signal is most likely from concerted triple dissociation as shown below, which has been suggested in the literature<sup>1</sup> although it was thought not to be a major channel



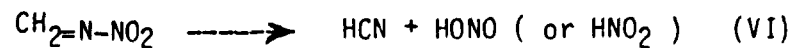
The  $P(E_T)$  for reaction (IV) is presented in figure 6. To fit the data it is assumed that the three product molecules have the same recoil velocity distribution in the C.M. coordinate system so that the average translational energy released in the dissociation is three times that of one  $\text{CH}_2\text{NNO}_2$ . More evidence to support mechanism (IV) will be given in the discussion section.

Using only reactions (I) - (IV) we can not completely fit the TOF spectrum of  $m/e = 46$  ( $\text{NO}_2^+$ ), specifically the fast edge which can not be attributed to any products from reactions (I) - (IV), indicating that there must be another dissociation channel which needs to be considered as will be shown later. Also, reactions (I) - (IV) can not fit the fast part of the TOF spectrum of  $m/e = 44$  which is most likely  $\text{N}_2\text{O}^+$  and must be explained by a secondary concerted dissociation channel. To determine the partner of  $\text{N}_2\text{O}$ , we inspected the possibility of producing  $\text{N}_2\text{O}$  together with  $\text{H}_2\text{CO}$  from  $\text{CH}_2=\text{N}-\text{NO}_2$  through reaction (V)



$\text{H}_2\text{CO}$  can give signal at  $m/e = 30, 29$  and  $28$ , of which  $30$  and  $28$  may not be solely due to  $\text{H}_2\text{CO}$  whereas  $29$  can only be explained by the formation of  $\text{HCO}^+$  from  $\text{H}_2\text{CO}$ . It is found that based on reaction (V) the fast parts of the  $m/e = 44$  and  $29$  spectra match each other well according to momentum conservation, indicating that (V) is indeed responsible for the production of  $\text{N}_2\text{O}$  and  $\text{H}_2\text{CO}$ . The  $P(E_T)$  for reaction (V) used in the data analysis is shown in figure 7, the high average translational energy being consistent with that expected for a concerted reaction.

Like that of  $m/e = 17$  ( $\text{OH}^+$ ), the TOF spectrum of  $m/e = 26$  ( $\text{CN}^+$ ) strongly indicates another secondary concerted reaction channel. By studying the TOF spectra of  $m/e = 28, 27$  and  $26$ , we concluded that this concerted dissociation channel gives  $\text{HCN}$  as one of its products. Recalling the problem remaining in fitting the fast component of the  $m/e=46$  ( $\text{NO}_2^+$ ) TOF spectrum, we are led to assign this channel as



Reaction (VI) can match both the  $m/e = 26$  and the fast component in the  $m/e = 46$  TOF spectra well through momentum conservation, and figure 8 shows the  $P(E_T)$  for reaction (VI) used to fit the TOF data.

The counterpart of HCN, which has a mass number of 47, in reaction (VI) is most likely to be HONO, but there are two observations which raise questions on this assignment. One is that Wodtke et al.<sup>7</sup> have shown that HONO produced from the IRMPD of nitroethane and nitropropane does not give appreciable amounts of  $\text{NO}_2^+$  and this is also true for HONO from reaction (II) (this product is so fast that one can not fit the fast component in the  $m/e = 46$  TOF spectrum by it), but the 47 in reaction (VI) contributes quite a bit of  $m/e = 46$ . Another is that when analyzing the  $m/e = 15$  TOF data, we found that none of products from the channels considered could match the fastest component which arrived at the detector about the same time as the fast component at  $m/e = 46$ . If the 47 is assigned as  $\text{HNO}_2$ , a more unstable intermediate which can give  $m/e=15$  ( $\text{HN}^+$ ) as well as  $m/e=46$  ( $\text{NO}_2^+$ ) in the ionizer, both problems disappear. We cannot tell at this stage which isomer is more likely and it is possible that both species are produced.

When reactions (I) -- (VI) are considered together with appropriate branching ratios, all of the observed TOF spectra can be fitted well. In order to provide further verification of the assignment given above we have carried out a comparison of mass spectra of the products. In Table I the relative yield of parent and daughter ions of some products measured in this experiment and those from the literature are compared. Because the molecules produced in the decomposition of RDX are internally hot, it is not surprising that more smaller fragments are produced from the dissociation products than from the same molecules at room temperature. Comparison shows that the mass spectra of most of these

species are in agreement with those in the literature. For  $N_2O$  the discrepancy seems large. This could be due to errors in fitting the data since  $N_2O$  is a small component, or it could be due to the really large difference in the cracking patterns between vibrationally hot  $N_2O$  and room temperature  $N_2O$  such that more  $m/e = 28$  ions are produced from  $N_2O$  in the decomposition of RDX.

Table II shows the results we have obtained for the laser power dependence of the signal level. Because the relative yields of products are nearly independent of laser power and the dependence of signal level on laser power is much less sensitive than one might expect, it is reasonable to assume that the primary dissociation processes are nearly saturated at  $20 \text{ J/cm}^2$  and that the secondary dissociations are mainly spontaneous dissociations rather than secondary photo-dissociations. More evidence for this will be presented later when RRKM dissociation rate constants are calculated.

## V. DISCUSSION

Among many possible decomposition schemes tested to explain our experimental observations the scheme of reactions (I) - (VI) gives the most satisfying results, but we cannot unambiguously conclude that they are the only reactions involved for the following reasons. First, there are too many components in most of the TOF spectra, the fit becomes more ambiguous for the minor components; second, the proposed reactions have many products with velocity distributions which are quite similar due to

the symmetric structure of RDX and it is possible that some minor reaction channels have not been identified. Nevertheless, we believe that this scheme includes the most important unimolecular channels involved in RDX decomposition.

#### A. BRANCHING RATIOS

In the decomposition of RDX, competition between parallel dissociation channels was found to take place in both primary and secondary reactions. In spite of the fact that determining the relative yields of products and branching ratios involving minor components is quite difficult, it provides another way of checking the reliability of the dissociation mechanism.

Table III lists the calculated relative product flux for various products. The theoretical and mathematical details for the calculation of branching ratios as well as fitting the TOF data where secondary reactions are involved will be presented in another paper<sup>10</sup>.

As shown, among the primary channels the reaction rate for concerted reaction (IV) is about twice that for simple bond rupture (I), that is, for each molecule of  $\text{NO}_2$  and 176 produced (from channel (I)), there are six  $\text{CH}_2=\text{N}-\text{NO}_2$  produced. The secondary dissociation branching ratios again show the domination of concerted channels as can be seen when products from reactions (II) and (III) are compared. In the secondary dissociation of  $\text{CH}_2=\text{N}-\text{NO}_2$ , the channel producing HCN is found to be more important than the channel producing  $\text{H}_2\text{CO}$  and  $\text{N}_2\text{O}$ . It is also seen that most of the unstable products from the primary channels dissociate so that only a small percentage of them remain intact.

By adding up all the products which are initially formed as 176, including those which survive and those which undergo further dissociation, we have obtained a ratio of 0.90 for 176 to 46 from reaction (I), compared to the expected value of 1.00. The measured ratio of 129 to 47 from reaction (II) is 0.80. When similar comparisons are made on other channels, it is found that the agreement between measured and desired ratios of the products is not always as good as that shown above, though the uncertainty is relatively large. Nevertheless, the reasonably good agreement in the ratios of products for the important channels give us confidence in our suggested mechanism.

#### B. THE SOURCE OF $\text{CH}_2\text{NNO}_2$

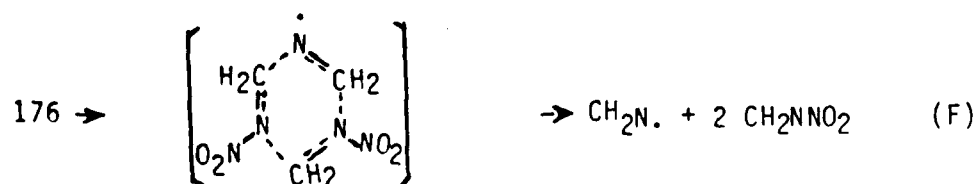
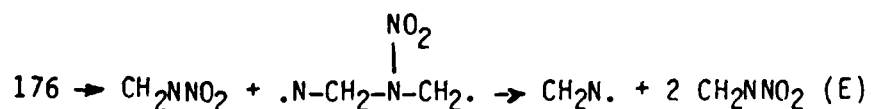
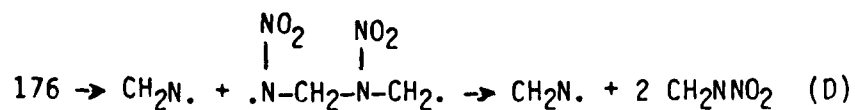
The species  $\text{CH}_2\text{NNO}_2$  (74) as an unstable intermediate in the decomposition of RDX has been recognized,<sup>1-3,9</sup> but there exists much speculation as to its origin. We have concluded that reaction (IV) is the main source of 74, because only this reaction can best explain our experimental observations, but according to theoretical calculations of Melius and Binkley<sup>3</sup> it is a very unlikely channel to compete with reaction (I).

Melius and Binkley<sup>3</sup> have estimated that the heat of formation of  $\text{CH}_2\text{NNO}_2$  is 33.6 kcal/mol, therefore the endothermicity of reaction (IV) would be about 80 kcal/mol. If the N-N bond energy in RDX is assumed to be 45 kcal/mol, then the excitation barrier for reaction (IV) would be at least 35 kcal/mol higher than that for reaction (I). The question naturally arises : can the molecule be pumped by laser excitation to such high energy levels while reaction channel (I) is

competing? To answer this question the unimolecular constants were calculated using RRKM theory. The calculations show that the RRKM rate constant for reaction channel (I) is only on the order of  $10^6 \text{ sec}^{-1}$  even when the total energy in the molecule reaches 100 kcal/mol. Using a program developed by Schulz<sup>11</sup> one can calculate the total internal energy distribution of the molecules by IRMPE pumping, and using this information on the internal energy distribution one can then calculate the translational energy  $P(E_T)$  distribution for the simple bond rupture channel using RRKM theory. From a comparison between the calculated and the observed translational energy distribution, the average total internal energy can be derived.<sup>7</sup> The average total internal energy of the molecule after the laser pulse was calculated around 80 kcal/mol. These results imply that the dissociation of the molecule through reaction channel (I) in this environment will not limit the excitation of the molecule by  $\text{CO}_2$  laser up-pumping (the laser pulse is shorter than 800 nsec) and since the internal energy distribution of excited molecules is similar to that from thermal excitation, reaction (IV) is energetically accessible for a large fraction of the RDX in this experiment even though the endoergicity derived from the heat of formation of  $\text{CH}_2\text{NNO}_2$  given by Melius and Binkley seems unreasonably high. These results also mean that most of the RDX dissociate after the laser pulse, and therefore it is almost certain that secondary dissociations are indeed spontaneous dissociations instead of secondary photo-dissociations during the laser pulse. . The domination of reaction

(IV) over reaction (I) indicates that either the heat of formation of  $\text{CH}_2\text{NNO}_2$  estimated by Melius and Binkley is too high or the experimentally provided heat of formation of RDX is too low, or the preexponential factor of reaction (IV) is substantially higher than that of reaction (I).

Melius and Binkley<sup>3</sup> suggested that one of the important reaction paths following reaction (I) may be that 176 undergoes a series of dissociation steps to give  $\text{CH}_2\text{N}$  and  $\text{CH}_2\text{NNO}_2$ . We have carefully studied this suggestion assuming the following mechanism, which through various steps forms one  $\text{CH}_2\text{N}$  and two  $\text{CH}_2\text{NNO}_2$ :



Due to the similarity of the products one can not absolutely eliminate the possibility that those reactions occur in the experiment, but we have observed no evidence for the existence of the intermediates in reactions (D) and (E), e.g.,  $m/e = 148$  or a faster second component in TOF spectrum of  $m/e = 102$ . In fact, reactions (D) and (E) are energetically unfavorable because starting with about 80 kcal/mol of internal energy, formation of  $176 + \text{NO}_2$  has consumed about 45 kcal/mol, and there is simply not enough energy for the molecule to split further to form the more unstable radical species. Also, in reaction (D),  $\text{CH}_2\text{N}$  product would give a very fast component in the  $m/e = 28$  TOF spectrum by momentum conservation, and reaction (E) would likely present two components in the TOF spectra of  $m/e = 74$  because the two 74 species in reaction (E) would have different velocity distributions, all of which are not consistent with the experimental observations. To check reaction (F), more careful work is needed, since theoretically it is possible for reaction (F) to produce fast signal at  $m/e = 74, 28, 27$  and  $26$ , and there is a simultaneous three body fission involved which makes analysis laborious. If reaction (F) was a main channel, we would expect that  $\text{CH}_2\text{N}$  would be responsible for the fast components in the TOF spectrum of  $m/e = 28, 27$  and  $26$ . In order to fit the data, we have chosen several different effective masses to represent approximately two 74 fragments together and found that the shape of the  $m/e = 74$  peak was too narrow to match that of  $m/e = 26$ . The shape of the fast edge of the  $m/e = 28$  TOF spectrum is different from that of  $m/e = 27$  and  $26$ , which also indicates that those signals are not mainly from  $\text{CH}_2\text{N}$  and reaction (F) is not

important, if it occurs at all. We also checked the possibility of producing 74 from further dissociation of the product which appears as the fast component in the  $m/e = 81$  TOF spectrum, and found that we cannot fit the  $m/e = 74$  spectrum even by using an unrealistically narrow  $P(E_T)$ , ruling out the possibility of 74 being formed from any larger products detected in this experiment. The most compelling evidence against reactions (D) - (F) is the branching ratio. If 74 was produced after reaction (I), we could at most obtain a ratio of 2:1 for  $\text{CH}_2\text{NNO}_2$  to  $\text{NO}_2$  from (I), but in fact we obtained a ratio of 6 and the lowest bound of this value is still larger than 2 even considering the worst possible uncertainties. Also, the ratio of 176 to  $\text{NO}_2$  from (I) is 0.90, consistent with the picture that most of the 74 is not from further dissociation of 176.

#### C. THE IMPORTANCE OF CONCERTED REACTION

The bulk thermal decomposition of RDX must contain both unimolecular and bimolecular processes. Since this experiment has eliminated the possibility of bimolecular reactions, the important unimolecular reactions involved are clearly revealed, even though it cannot answer all questions about the thermal decomposition of RDX. From the experimental results we have seen that unimolecular dissociation processes play important roles, especially in the initial steps. Comparing the distribution of products observed in this experiment with that from thermal decomposition<sup>1</sup> we can say that unimolecular dissociation is indeed the main avenue even for bulk RDX decomposition, because

sequential unimolecular dissociations are responsible for the major products observed in thermal decomposition.

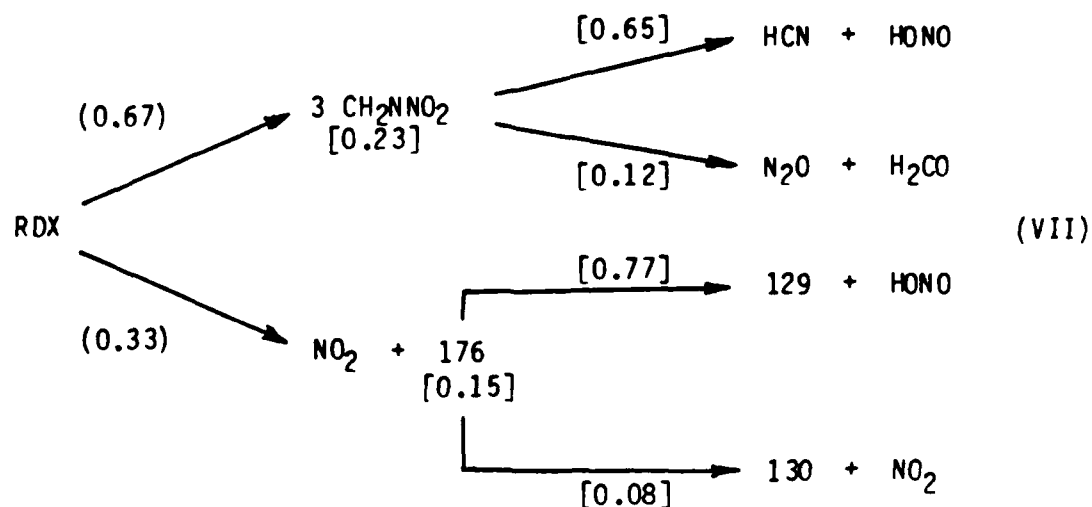
There have been many reaction channels proposed for the thermal decomposition of RDX,<sup>1-4</sup> most of which are simple bond rupture or bimolecular processes. Our experiment has shown that through concerted unimolecular dissociation channels RDX goes to various final products similar to those of bulk dissociation in only two steps. For simple bond rupture the potential energy surface of the molecule usually has a high activation energy with at most a small exit barrier. Most of the energy is either consumed to break the chemical bond or tied up in vibrational degrees of freedom, so that only a small amount of translational energy is released. In contrast, in concerted reactions the molecule usually has a strained configuration at the transition state, and after crossing this barrier to form products, much of the extra potential energy of the transition state appears in the form of repulsion between the recoiling partners, that is, in the form of translational energy.

If the main reaction paths in the thermal decomposition of RDX were through bimolecular reactions, the bulk product distribution would be even more complicated than it is, because there are many possible ways for the unstable intermediates and radicals to combine with each other. It has been shown that at low temperatures the two most probable products of thermal decomposition of RDX are  $N_2O$  and  $H_2CO$  ( $195^\circ C$ ) which decrease as the temperature increases, while at high temperature ( $600^\circ C$ )  $HCN$  and  $NO$  become the two largest products,<sup>1</sup> consistent with the concerted reaction picture presented here. In this experiment among

six observed reaction channels only two occur through simple bond rupture and, as seen above, their relative amounts are small. Concerted reaction is dominant not only in the number of channels but also in the amount of products formed.

Knowing the branching ratios, we can answer another interesting question, that is, how many molecules are produced and how much energy is released into translation per RDX molecule within this scheme. It is calculated that there are 4.5 molecules produced on average compared with bulk thermal decomposition where the average number of molecules produced is 7.<sup>12</sup> Obviously, in the case of thermal decomposition some of the products which are formed in IRMPD will undergo further reaction through either unimolecular or bimolecular paths and all of the unstable intermediates will be eventually converted into stable products.

In this experiment 26.4 kcal/(mol RDX) was released to translation in the C.M. frame of RDX. Although part of this energy is from the CO<sub>2</sub> laser, it helps us to think about the case of bulk thermal decomposition, where activation of the molecules is by thermal energy and after endothermic initial steps further exothermic steps follow. Based on the thermochemical data given by Melius and Binkley<sup>3</sup> and the branching ratios obtained in this paper the endothermicity of reaction



is 32 kcal/(mol RDX) and the average internal energy of RDX is about 80 kcal/mol as shown before. Therefore over half of the available energy appears in translation. The normalized branching ratio of the primary dissociation steps are shown in parentheses. For the secondary dissociations, the three numbers shown in brackets for each branch are the relative amount of those remaining as primary products and the two secondary reaction channels.

## VI. SUMMARY

IRMPD in a molecular beam with its unique advantage has been successfully used to study unimolecular dissociation. This method has been extended to even larger molecules and much more complicated processes than before, where its advantages become even more appreciable. We have shown that it is possible to get enough RDX into the gas phase for molecular beam studies. We have also shown that RDX easily undergoes

multi-step unimolecular dissociation. There are many channels competing with each other, with concerted dissociation dominant manner, allowing very simple products such as HCN,  $H_2CO$  and  $N_2O$  observed in bulk thermal decomposition, to be produced in a few steps and a short time. We have observed a concerted triple dissociation channel which is one of only a few that have been found so far.<sup>13</sup> It is worthwhile paying more attention to these dissociation mechanisms both experimentally and theoretically due to their importance in the dissociation of highly symmetric polyatomic molecules and their fascinating nature. A fair amount of translational energy release through concerted reaction has been observed, which is significant for explaining the nature of the energy release in RDX decomposition.

#### ACKNOWLEDGEMENTS

The authors are thankful to A. M. Wodtke for his help throughout this study and to H. Hornig at Lawrence Livermore Laboratory for providing the RDX sample. This work was supported by the Office of Naval Research under Contract No. N00014-83-K-0069.

REFERENCES

1. M. A. Schroeder has written a series of review articles, of which we quote most frequently M. A. Schroeder, Proceedings, 18th JANNAF Combustion Meeting, Vol. II, 395 (1981).
2. J. J. Batten, Int. J. Chem. Kinetics, 17, 1085 (1985).
3. C. F. Melius and J. S. Binkley, submitted for publication.
4. S. Bulusu, D. I. Weinstein, J. R. Autera and R. W. Velicky, J. Phys. Chem., 90, 4121 (1986).
5. D. Krajnovich, F. Huisken, Z. Zhuang, Y. R. Shen and T. Y. Lee, J. Chem. Phys., 77, 5977 (1982).
6. L. J. Butler, R. J. Buss, R. J. Brudzynski and Y. T. Lee, J. Phys. Chem., 87, 5106 (1983).
7. A. M. Wodtke, E. J. Hintsä and Y. T. Lee, J. Phys. Chem., 90, 3549 (1986).
8. A. M. Wodtke and Y. T. Lee, J. Phys. Chem., 89, 4744 (1985).
9. M. Farber and R. D. Srivastava, Chem. Phys. Lett. 64, 307 (1979).
10. G. Nathanson, X. Zhao and Y. T. Lee, to be published.
11. a) E. R. Grant, P. A. Schulz, A. S. Sudbo, Y. R. Shen and Y. T. Lee, Phys. Rev. Lett., 40, 115 (1978). b) P. A. Schulz, Ph. D. thesis, University of California (1979).
12. J. J. Batten, Aust. J. Chem., 24, 945 (1971).
13. a) A. C. Scheiner, G. E. Scuseria and H. F. Schaefer III, J. Am. Chem. Soc., 108, 8160 (1986). b) X. Zhao, W. B. Miller, E. J. Hintsä, and Y. T. Lee, to be published.

Table I  
Comparison of Mass Spectra<sup>a</sup>

<u>species</u>	<u>m/e</u>	<u>relative amount</u>		<u>species</u>	<u>m/e</u>	<u>relative amount</u>	
		<u>this work</u>	<u>lit.</u>			<u>this work</u>	<u>lit.</u>
NO <sub>2</sub> (I)	46	335	370	NO <sub>2</sub> (II)	46	612	370
	30	1000	1000		30	1000	1000
	16	429	223		16	290	223
	14	117	96		14	80	96
N <sub>2</sub> O	44	131	1000	H <sub>2</sub> CO	30	174	600
	30	187	311		29	160	1000
	28	1000	108		28	1000	307
	16	27	50		16	55	18.8
	14	7	127		14	53	15.3
HCN	27	1000	1000	13	82	8.2	
	26	70	168	12	80	8.2	
	14	29	11				
	13	5	17				
	12	21	17				

a Literature values in this table are from Atlas of Mass Spectral Data, edited by E. Stenhagen, S. Abrahamsson and F. W. McLafferty, Vol. I, Interscience Publishers (1969).

Table II  
Experimental laser power dependence of signal counts  
in ions per laser shot

<u>m/e</u>	<u>lab. angle(°)</u>	laser power in J/cm <sup>2</sup>		
		<u>20</u>	<u>16</u>	<u>6</u>
30	14	32.0		16.0
74	10	1.55		1.04
74	14	1.31		0.93
42	14	2.52		1.67
17	14	0.14	0.13	
102	10	1.24	1.07	

Table III  
Relative Total Product Flux<sup>a</sup>

		<u>primary</u>			
species	46(I)	176(I) <sup>b</sup>		74(IV) <sup>b</sup>	
relative flux	1.0 <sup>c</sup>	0.90		6.1	
		<u>secondary 1, from 74</u>			
species	27(VI)	47(VI)	44(V)	30(V)	74(IV) <sup>d</sup>
relative flux	5.4	2.6	1.0 <sup>c</sup>	1.5	1.9
		<u>secondary 2, from 176</u>			
species	129(II)	47(II)	130(III)	46(III)	176(I) <sup>d</sup>
relative flux	9.6	12	1.0 <sup>c</sup>	4.3	1.9

a (I) - (VI) stand for the reaction channels in the text, and the number stands for the species of that molecular weight.

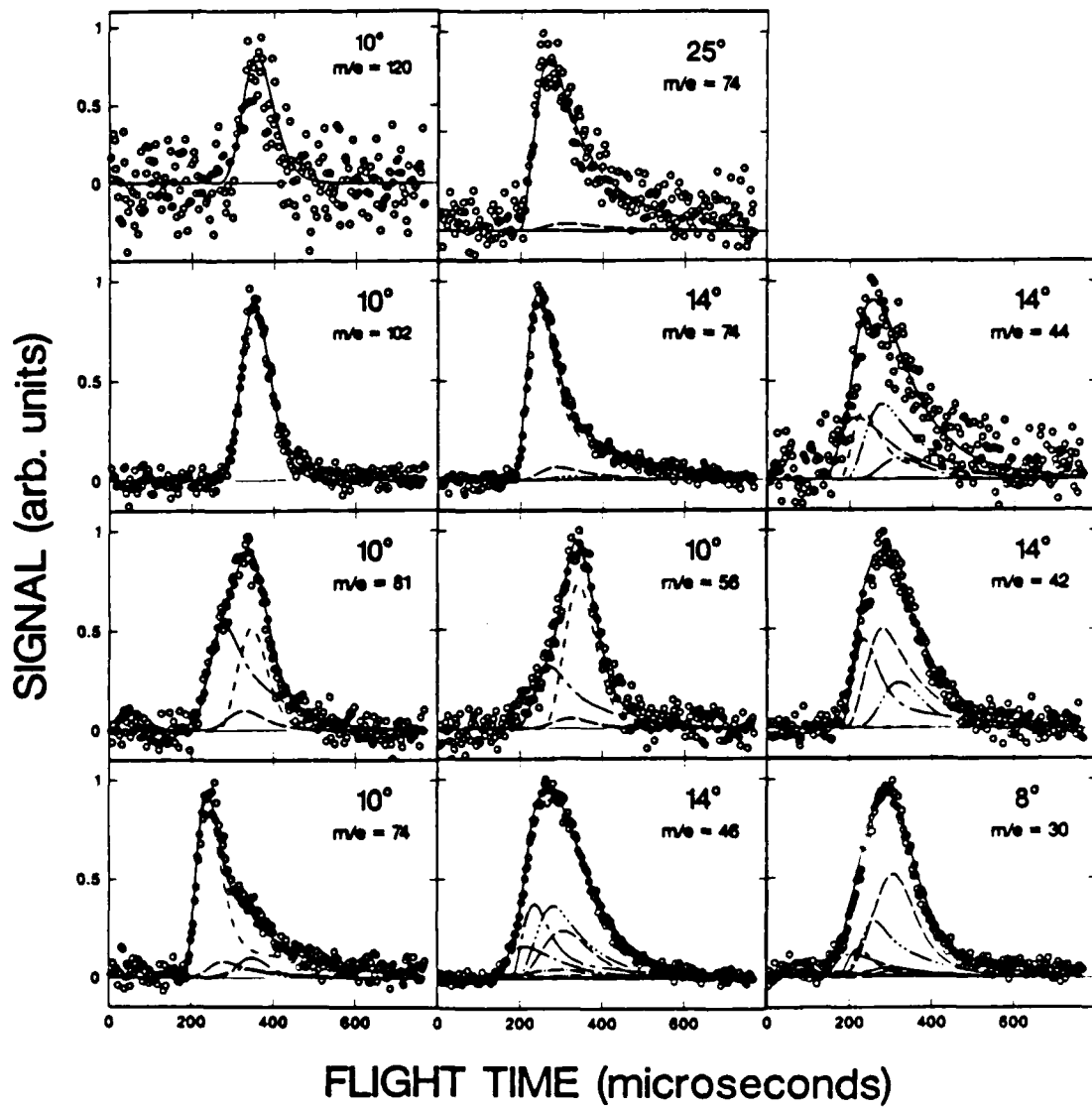
b sum of those undergoing secondary dissociation and those which survive.

c chosen as 1.0.

d only those which survive.

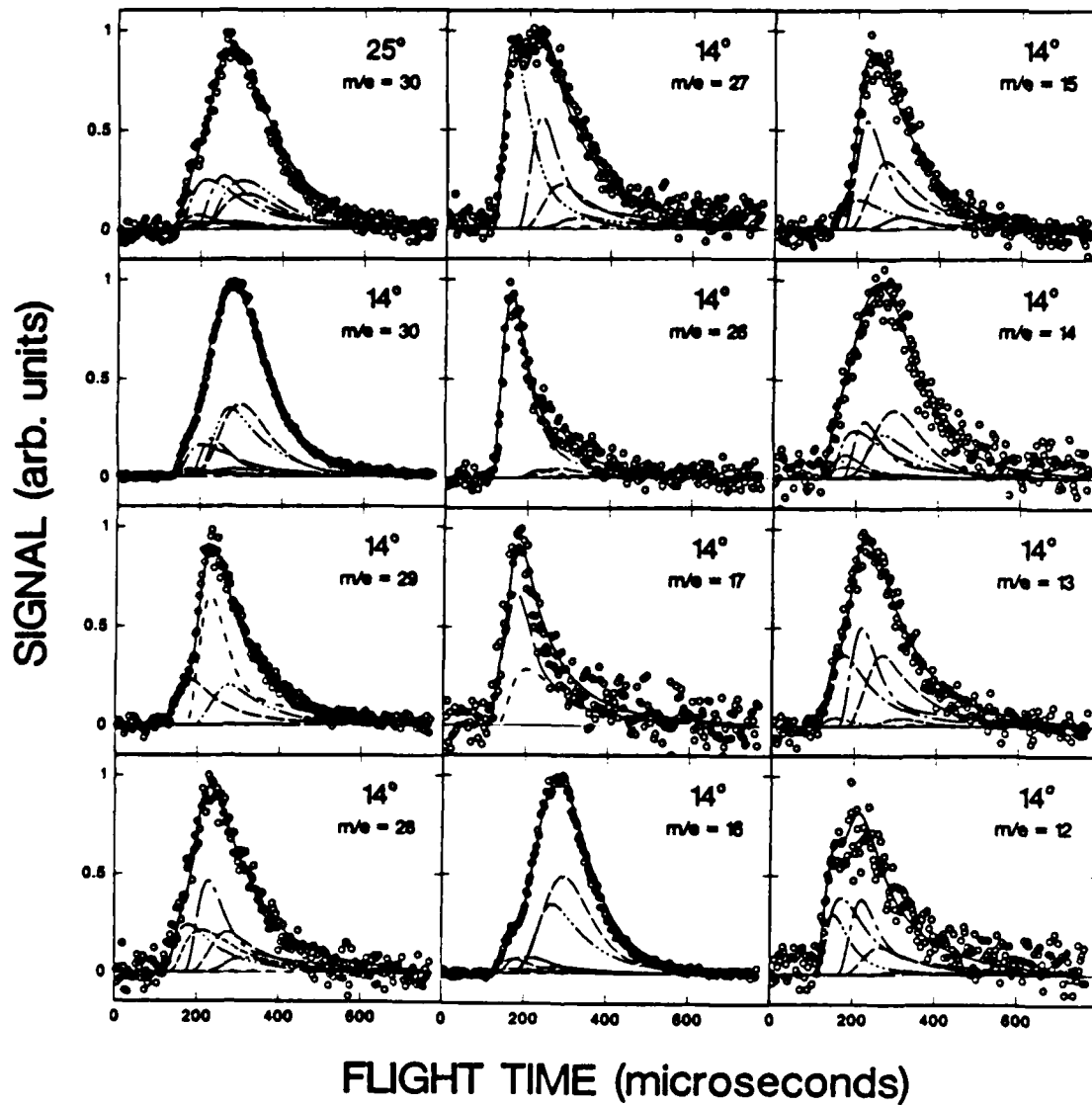
FIGURE CAPTIONS

- Fig. 1 TOF spectra for the masses with  $m/e$  greater than 30. The open circles are observed data and the curves are calculated TOF spectrum. The angle in each TOF spectrum is the laboratory angle at which the spectrum was taken.
- Fig. 2 TOF spectra for the masses with  $m/e$  smaller than 30. The open circles are observed data and the curves are calculated TOF spectrum. The angle in each TOF spectrum is the laboratory angle at which the spectrum was taken.
- Fig. 3  $P(E_T)$  for reaction (I) used to fit experimental data in figs. 1 and 2.
- Fig. 4  $P(E_T)$  for reaction (II) used to fit experimental data in figs. 1 and 2.
- Fig. 5  $P(E_T)$  for reaction (III) used to fit experimental data in figs. 1 and 2.
- Fig. 6  $P(E_T)$  for reaction (IV) used to fit experimental data in figs. 1 and 2.
- Fig. 7  $P(E_T)$  for reaction (V) used to fit experimental data in figs. 1 and 2.
- Fig. 8  $P(E_T)$  for reaction (VI) used to fit experimental data in figs. 1 and 2.



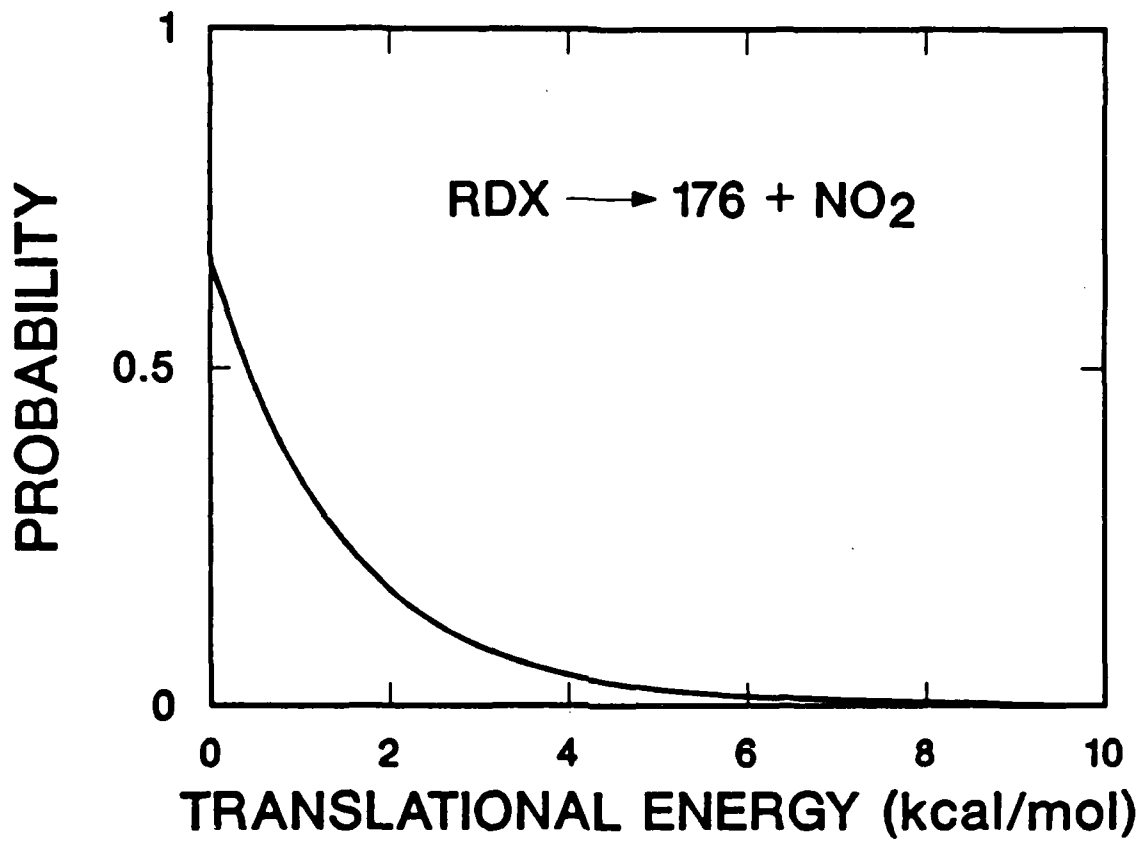
XBL 375-2319

fig. 1



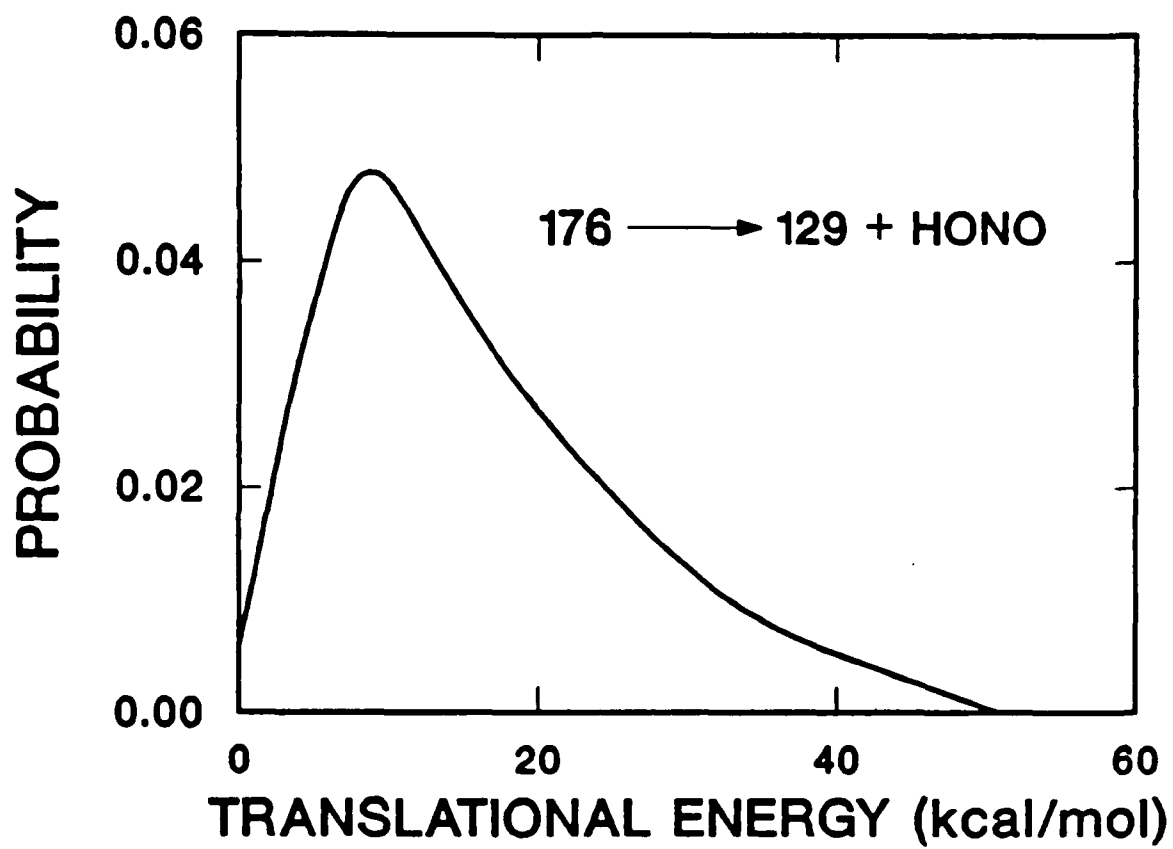
XBL 875-2318

fig. 2



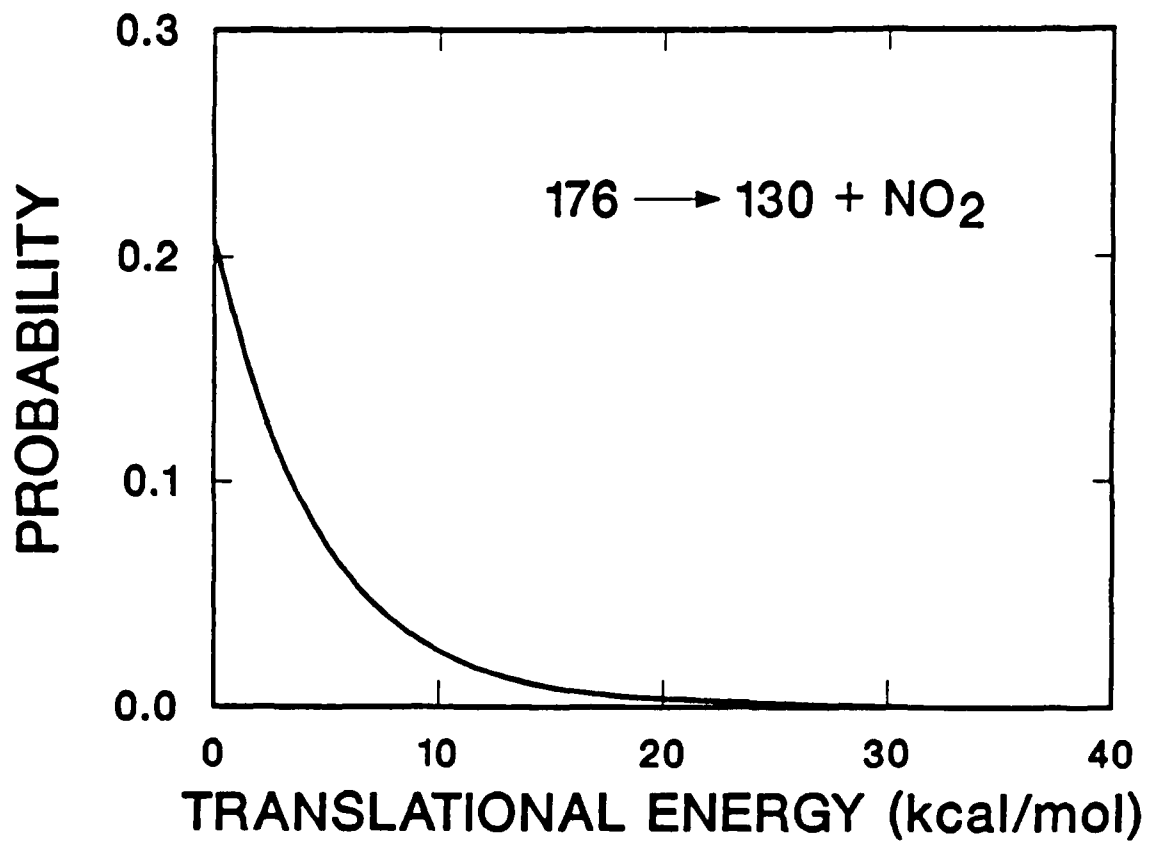
XBL 875-2325

fig. 3



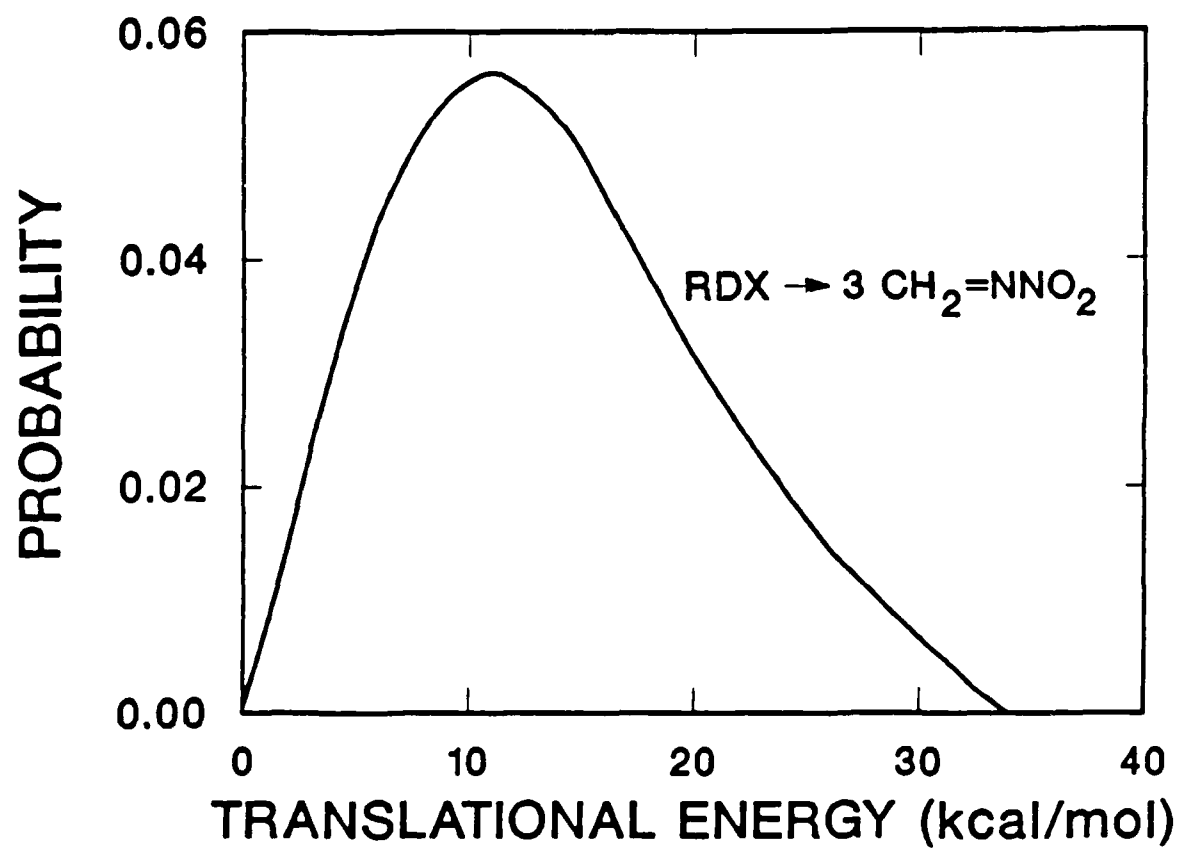
XBL 875-2323

fig. 4



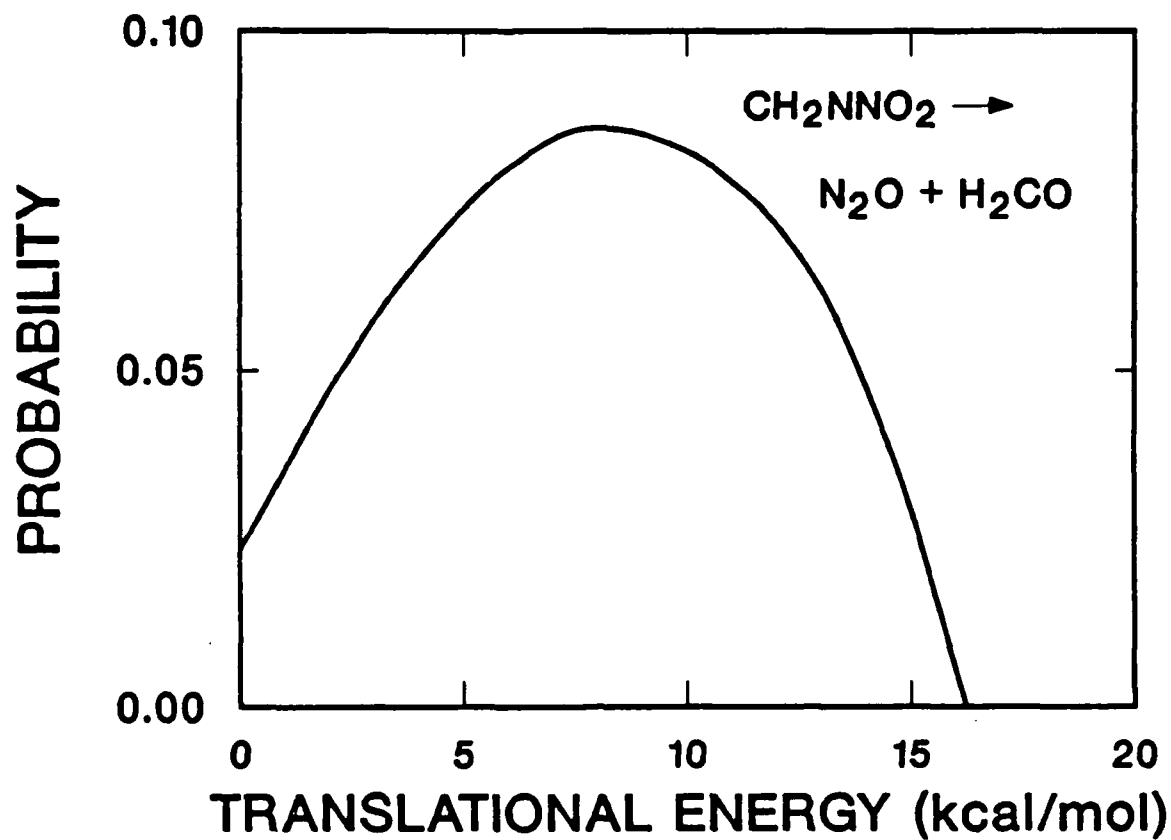
XBL 875-2324

fig. 5



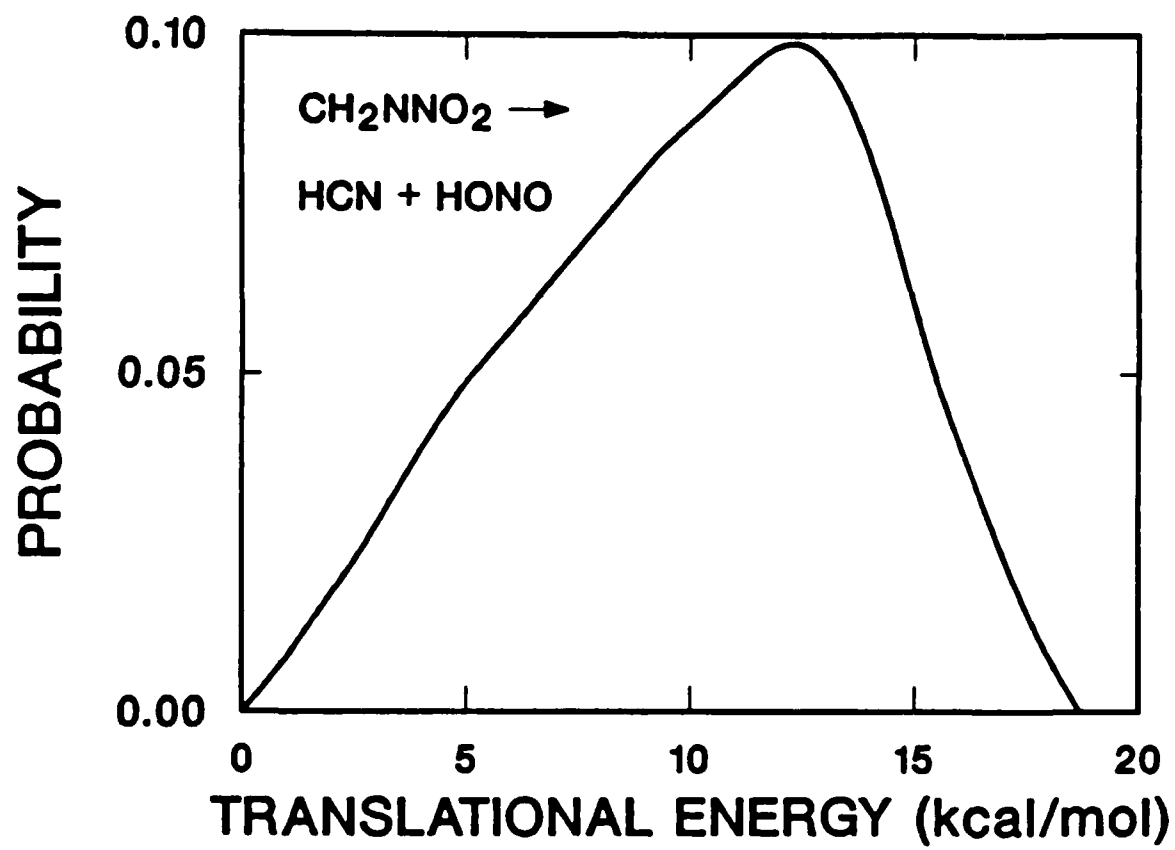
XBL 875-2320

fig. 6



XBL 875-2321

fig. 7



XBL 875-2322

fig. 8

END

9-87

DTIC